



A spatial simulation approach to hydroacoustic survey design: A case study for Atlantic menhaden



Dong Liang*, Geneviève M Nesslage, Michael J Wilberg

University of Maryland Center for Environmental Science, Chesapeake Biological Laboratory

ARTICLE INFO

Handled by George A. Rose

Keywords:

Omni-directional sonar
Biomass estimation
Effort allocation
Forage fish
Informative sampling
Survey strategy

ABSTRACT

Patchily distributed pelagic fish species present a challenge to classical approaches to hydroacoustic survey designs. We propose a spatial simulation approach to designing acoustic surveys and provide a case study in the northern resident stock of Atlantic menhaden *Brevoortia tyrannus* during winter. The structure and abundance of this stock is poorly characterized due to a paucity of fishery-independent surveys and the geographically limited range of the reduction fishery. In order to develop new fishery-independent information for this stock, we conducted a simulation study to estimate the accuracy and precision of an offshore hydroacoustic survey. We simulated a spatial super-population based on fishery-dependent data, and randomly re-sampled the population with various types of hydroacoustic survey equipment. Our results suggest that a combination of down-viewing echosounder and omni-directional sonar can generate biomass estimates with a coefficient of variation around 25%. The use of down-viewing echosounder alone, however, generated biomass estimates with poor precision. Our approach accounts for the patchy spatial distributions of the survey populations, which leads to more realistic estimates of precision than classical approaches implicitly assuming independence. The approach also evaluates several types of hydro-acoustic survey equipment in deriving absolute biomass estimates, and the survey, once implemented, may contribute to improved spatially explicit management of the stock.

1. Introduction

Hydroacoustic (termed acoustic hereafter) surveys are a useful technique in fishery research for estimation of stock biomass or abundance (Simmonds and MacLennan, 2005). For example, acoustic surveys enable monitoring of pelagic clupeid populations at a sufficient spatiotemporal resolution to inform stock assessment and management (De Oliveira and Butterworth, 2004; Zwolinski et al., 2012). Surveys currently used to assess pelagic clupeid stocks along the continental shelf include herring in the USA and Europe (Overholtz et al., 2006; Simmonds, 1996), sprat in the UK (Casini et al., 2011), and sardines along the West Coast of the USA (Demer et al., 2012, 2013; Zwolinski et al., 2012). A line-transect design was used to acoustically survey these populations, with transects randomly selected using either stratified or systematic designs to achieve precise biomass estimates (Jolly and Hampton, 1990; Simmonds and Fryer, 1996). Simulation testing was conducted in a super-population framework to characterize the precision of such sampling designs (Simmonds and Fryer, 1996), but none of these studies considered the detectability of acoustic systems such as down-ward viewing or side-scan sonar.

Spatial distribution of the stock and the properties of acoustic

survey equipment are two important components in the process of acoustic survey design (Simmonds and Fryer, 1996). However, approaches that ignore the spatial component, such as the degree of coverage, are still commonly used as guides for determining total length of transects for acoustic surveys (Aglen, 1989, Section 9.6.4 in Simmonds and MacLennan, 2005). When simulation studies are used to inform the design of acoustic surveys, they typically have focused on other survey components such as comparing estimators of abundance (Gimona and Fernandes, 2003), design type (e.g., stratified, systematic; Simmonds and Fryer, 1996), or how to deal with shapes and orientations of schools (Kalikhman and Ostrovsky, 1997). Ignoring the spatial distribution of schools may lead to less accurate estimates of abundance or biomass than is desired (Simmonds and MacLennan, 2005).

Pelagic clupeids typically form schools that can span hundreds of meters in length, resulting in a patchy spatial distribution of schools across the landscape (Boyd et al., 2014; Haugland and Misund, 2004). Simulation studies based on statistical models for the spatial distribution of the stock could account for the schooling behavior of the stock (Ch. 22, Thompson, 2012), but these approaches have rarely been applied to hydroacoustic surveys designs for pelagic clupeids. We therefore developed a spatial simulation approach that accounted for the

* Corresponding author.

E-mail address: dliang@umces.edu (D. Liang).

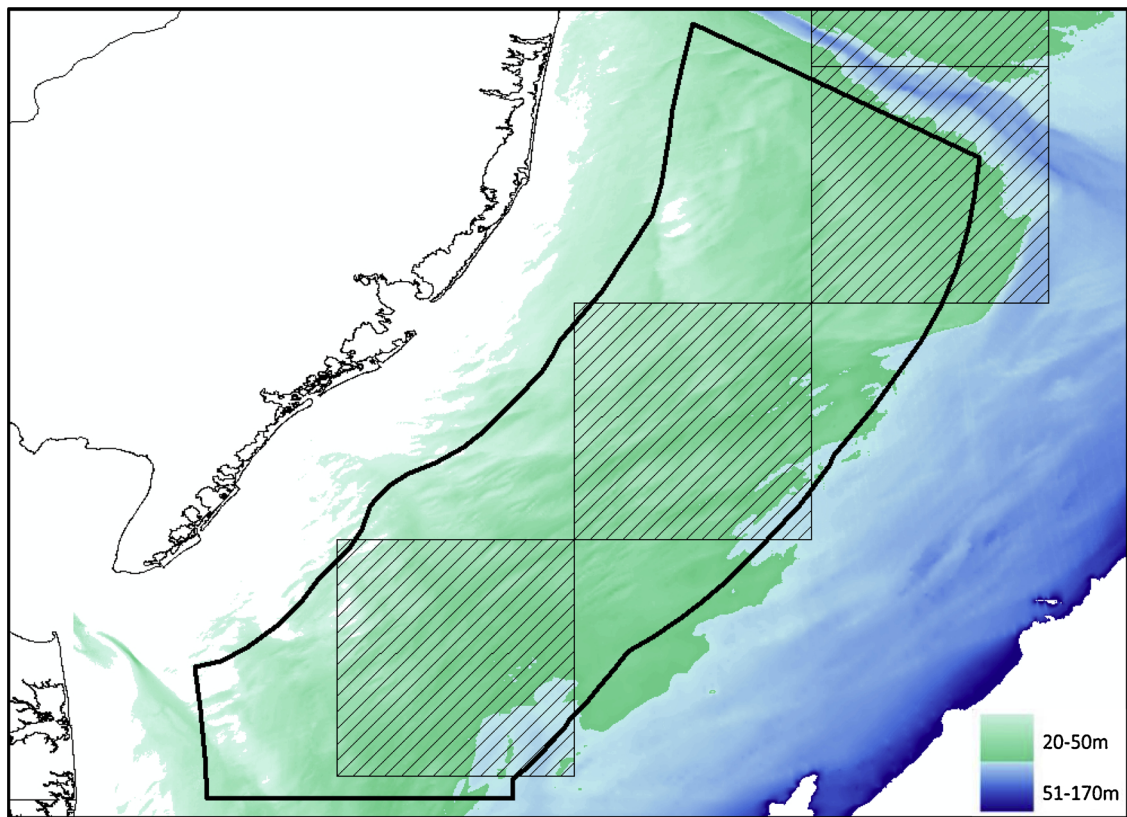


Fig. 1. Proposed survey area (black line) spanning 15–50 miles off the coast of New Jersey from the southern edge of Hudson Canyon extending southward to the New Jersey/Delaware border. Location of menhaden catch reported by Northeast Fisheries Observer Program between January and March, 2006–2016 (hatched squares) within the study area (black line). To maintain confidentiality, data are plotted by quarter degree square.

patchy spatial distribution of the stock and the properties of acoustic survey equipment. Specifically, our approach considered both traditional downward-facing echosounder designs and additional information provided by omni-directional sonar (Brehmer et al., 2006; Stockwell et al., 2012).

One such pelagic clupeid that forms large, patchily distributed schools is Atlantic menhaden *Brevoortia tyrannus*. The Atlantic menhaden stock supports the largest fishery by volume on the east coast of the USA with annual landings of 131 to 715 thousand metric tons (ASMFC, 2017). Menhaden were the focus of a purse-seine fishery that historically ranged from the Gulf of Maine to Florida. However, the geographical range of the purse-seine fishery has contracted since the 1980s and is now focused on the Chesapeake Bay and nearby coastal waters. Although menhaden are assessed as a single, coastwide stock (ASMFC, 2017), data from the northern portion of the species' range during winters has been sparse since the reduction fishery contracted. Currently, fisheries independent information on spatial distribution and biomass of menhaden outside the reduction fishery's range is limited to estuarine waters or a small portion of the coastal waters of New York (Lucca and Warren, 2018, 2019).

Several recent menhaden studies have changed our understanding of the species' life history in ways that might impact assessment and management. Until recently, scientists assumed that most spawning-age menhaden migrate south in winter to congregate offshore south of Cape Hatteras. However, recent re-analysis of historical tagging data indicates the presence of resident menhaden populations coastwide in winter (Liljestrand et al., 2019). Recent analysis of long-term ichthyoplankton survey data corroborates the year-round presence of spawning menhaden across the Mid-Atlantic (Simpson et al., 2017, 2016). Also, the recent development of a successful winter bait fishery on the offshore shelf of Southern New England provides additional evidence of the presence of resident adult menhaden in winter (SEDAR, 2015).

These new studies and fishery highlight the need to better characterize the spatial distribution and biomass of the northern resident menhaden stock in winter.

To adequately survey for menhaden, acoustic survey equipment and depth must be carefully considered. In most bottom trawl surveys, menhaden are captured at extremely low rates (SEDAR, 2015). Thus, an aerial survey has been proposed for monitoring menhaden when schools are located near the surface in late summer to early fall (Latour, 2013). However, an aerial survey will not suffice in winter because menhaden do not school at the surface between January and March and commercial fishers report offshore schools are located near the ocean floor (S. Axelsson, pers. comm., Ahrenholz, 1991; June and Reintjes, 1959; Reintjes, 1969; Smith, 1991). Acoustic equipment currently used by the fishing industry, namely a combination of downward-viewing echosounders and omni-directional sonar (Bernasconi et al., 2009; Brehmer et al., 2006; Stockwell et al., 2012), are more appropriate for surveying menhaden in winter because they operate over the entire water column. A combination of sonar and echosounder data collection can cover a larger volume of water in a limited amount of time (Brehmer et al., 2006; Fässler et al., 2016; Hewitt, 1976; Jones et al., 2017; Misund et al., 1995; Simmonds and MacLennan, 2005). Comparison of echosounder vs. sonar data collected from the same vessel indicates that sonar can encounter one to two orders of magnitude more school targets in the same amount of time (Hewitt, 1976).

The aim of this study is to illustrate the application of spatial simulation methods to the design of hydroacoustic surveys for a schooling species that exhibits a patchy spatial distribution. A case study application is provided to compare the precision of biomass estimates of Atlantic menhaden in the shelf waters off New Jersey in winter using several acoustic survey designs, and to justify the total transect distance to sample. Our analyses are based on limited fishery-dependent data from this region and season, published literature, and

local fisherman's knowledge. We begin by modeling the spatiotemporal super-population of the menhaden stock in this region and season. We then re-sample the simulated population according to the proposed designs and present the likely precision of the estimates.

2. Methods

2.1. Survey timing and study area

The survey area includes the region extending 15–50 miles offshore from the southern border of Hudson Canyon in the north to the New Jersey/Delaware border in the south (Fig. 1). This study area was chosen to represent the region off the New Jersey coastline in which the winter bait fishery for menhaden typically operates and menhaden bycatch in other fisheries is concentrated (Fig. 1). Also, the inshore limit was chosen so as not to overlap with winter tows of the New Jersey Ocean Trawl Survey (max extent ~13 miles offshore) and to focus on areas further offshore where adult menhaden are typically encountered (SEDAR, 2015). The offshore limit was defined as the approximate maximum distance reported in midwater trawl Vessel Trip Reports (VTRs, 2014–2017) and all Northeast Fisheries Observer Program (1989 and 2016) reports within the study area in winter which roughly follows the 50 m isobath (Fig. 1). The proposed survey would occur in February when water temperatures in the region drop to ~4–6°C and menhaden schools exhibit greatly reduced mobility (S. Axelsson, pers. comm., June and Reintjes, 1959).

2.2. Fishery-dependent and environmental data

A combination of fishery-dependent and environmental data was used to simulate the potential distribution of menhaden schools across the study area. Two sources of fishery-dependent menhaden data were available from the study region in the winter season to help inform simulations. The first data source was menhaden bait fishery Vessel Trip Reports provided by NOAA Fisheries Greater Atlantic Regional Office with permission of the fishermen spanning the start of the fishery in 2014 to 2017. Second, a logbook designed for this project (Supplement Table 1) was kept voluntarily by the fishermen during the 2018 winter fishing season to obtain information on schools encountered (location, depth, temperature, amount caught) and encounter rate (distance and time searched).

Monthly bottom temperature and salinity estimates were obtained from 0.2° monthly hydrographic climatology generated for the Mid-Atlantic Bight continental shelf (Richaud et al., 2016; <https://www2.who.edu/staff/ykwon/data>). Bathymetry data were obtained from NOAA's National Centers for Environmental Information U.S. Coastal Relief Model (<https://www.ngdc.noaa.gov/mgg/coastal/crm.html>). The existing environmental covariates were distributed at multiple spatial resolutions, resulting in spatial misalignments between the covariates. We aligned the environmental layers onto a common ~500 m resolution using the R package raster (Hijmans, 2017).

2.3. Sampling design

Given the lack of information about how menhaden utilize pelagic habitat in northern, offshore waters in winter, it was deemed better not to stratify than to incorporate inappropriate strata (Simmonds and Fryer, 1996; Simmonds and MacLennan, 2005). A systematic parallel design was chosen due to its superior performance for spatially structured populations (Overholtz et al., 2006). The survey area was first divided into parallel transects with major axes perpendicular to the shoreline (Fig. 2). Transect lengths varied due to the irregularly shaped survey area. A systematic random sampling design was chosen to select a fixed number of transects (Fig. 2) from five to twelve based on logistical constraints. Sample sizes (*i.e.* the number of transects and total transect length) were chosen based on the simulation study described

below.

Re-sampling was conducted according to seven strategies, assuming various detectabilities. We assumed that a vessel with mid-water trawl gear, downward-viewing echosounder and omni-directional sonar was available for the simulation design. Four sampling strategies with increasing expected costs were defined below.

- 1 Downward-viewing echosounder used to estimate biomass for each school encountered within a narrow athwartship (*i.e.* horizontal detection range of the down-looking echosounder) detection range of 20 m. This range (20 m) was chosen based on a beamwidth of 10° for the echosounder, and an average water depth of 50 m to represent the maximum detection range achievable in our study area; actual detection ranges achieved will be lower at shallower depths.
- 2 Downward-viewing echosounder (same as Option 1) used to estimate the biomass of each school encountered. In addition, omni-directional sonar is used to detect schools within 400 ms of each side of the vessel to estimate the number of additional schools encountered. The 400 m range was estimated based on the shallowest depth in the study area (20 m) and previous sonar surveys (Brehmer et al., 2007; Hewitt, 1976; Mackinson et al., 1999; Misund et al., 1995; Stockwell et al., 2012). The average biomass identified using the downward-viewing echosounder was multiplied by the number of schools identified by sonar to estimate the total biomass along each transect (Lucca and Warren, 2018).
- 3 Sonar used to identify locations of all schools within 400 ms each side of the vessel. Any school detected by the omni-directional sonar will be observed using the down-viewing echosounder to estimate biomass of each encountered school. Total biomass is aggregated based on all down-viewing estimates.
- 4 Sonar is used to identify menhaden schools, and each identified school along the transect is captured with mid-water trawl gear. Total biomass is measured dockside and aggregated based on the sum of biomass captured.

Options 5–7 are similar to options 2–4 except that a 200-meter detection distance each side of the vessel is assumed (instead of 400 ms) to examine survey design performance under less ideal conditions due to either survey logistical constraints or other unforeseen limitations on school detection.

2.4. Spatial distribution of schools – Poisson process model

Several features of the available commercial menhaden data pose challenges to a classical Point process model (Diggle, 2013). Specifically, the occurrences of menhaden schools encountered by fishermen are not randomly sampled, and they were observed over dynamic environmental conditions. We used a dynamic point process model to predict the presence of successful trips given environmental conditions. Specifically, we assumed that the fisheries data follow a dynamic Poisson process with intensity $\lambda(u, t)$ for any possible cruise location u in the study area S and time step t . S represents the hypothetical collection of all possible fishing locations,

$$\ln(\lambda(u, t)) = Z(u, t)^T \beta \quad (1)$$

The generic term $Z(u, t)$ is a vector of time-varying environmental covariates depending on location $u \in S$ and time t , and β denotes a vector of coefficients of interest.

We consider two specific models of (1). We denote bottom temperature, salinity, latitude and bathymetry as *sbt*, *sbs*, *lat* and *bathy* in Eqs. (2) and (3). Parametric linear (2) as well as additive trends (3) were fitted for each covariate during the fishery observation period.

$$\ln(\lambda) \sim \text{bathy} + \text{sbs} + \text{sbt} + \text{lat} \quad (2)$$

$$\ln(\lambda) \sim \text{bathy} + \text{sbt} + s(\text{lat}) \quad (3)$$

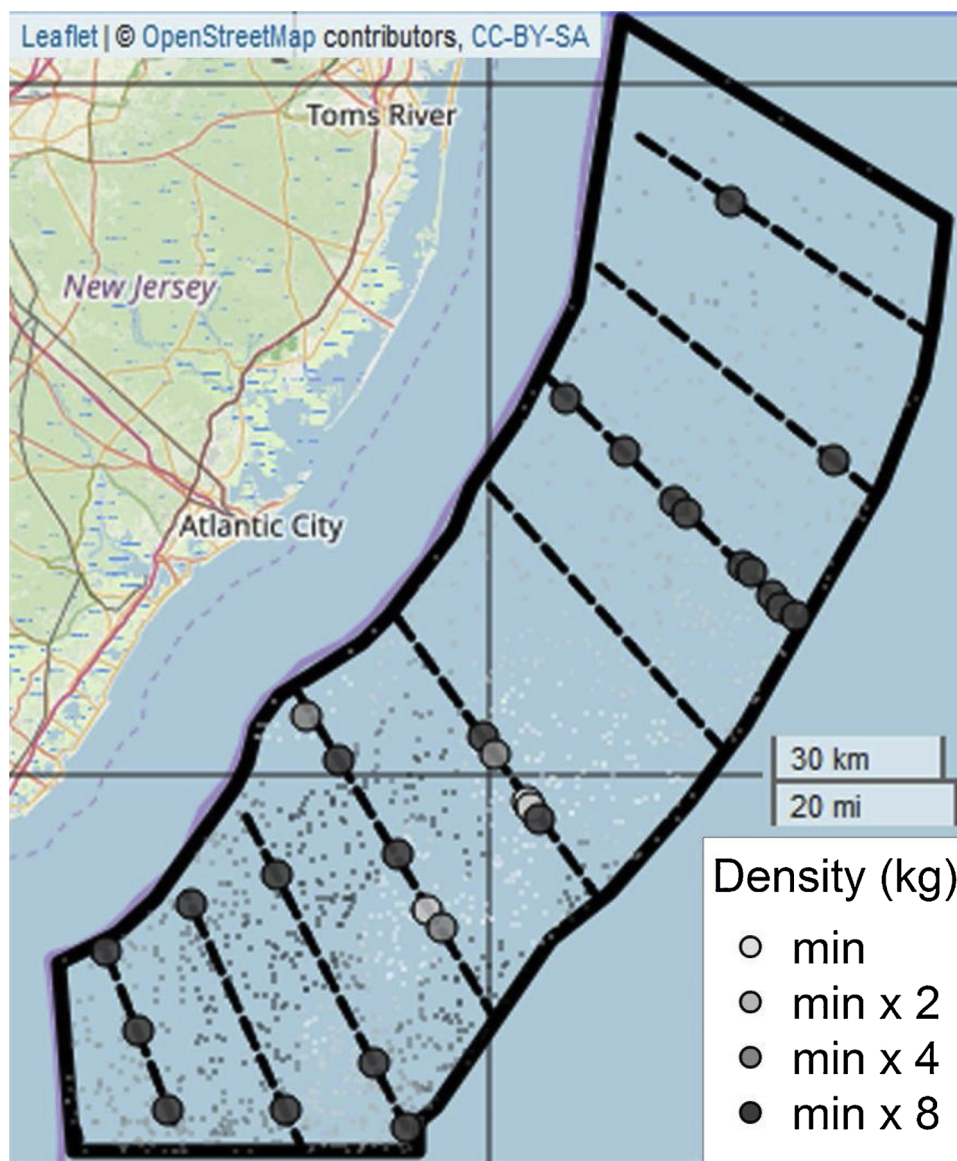


Fig. 2. An example sample of 10 transects using systematic sampling from a frame of 562 transects based on a 400 m omni-directional sonar detection range. Dark circles represent schools encountered within the detection distance. Simulated school density (kg) based on kriging observed Vessel Trip Reports catch per school were shown onto simulated school distribution. Magnitude of catches increase with darker colors, but are reported relative to the minimum density to protect confidentiality of industry data.

Model comparison was based on the Akaike Information Criterion. Statistical inference was based on a computational efficient approximation of the intractable dynamic Poisson process likelihood, implemented in the R package spatstat (Baddeley et al., 2015). The additive trends were estimated using the R package mgcv (Wood, 2011).

We simulated the spatial distribution of schools determined by the fitted Poisson process map representing the expected number of schools encountered per unit area under the dynamic Poisson point process model (Fig. 3). The VTR data were re-sampled to represent the hypothetical number of trips (*i.e.* re-sample size) required to catch the entire population. The re-sample size was determined based on fishery encounter rates with menhaden schools observed in the field.

2.5. School density – local kriging

Biomass per school encountered was determined by the distribution of observed fishery catches (Fig. 2). We used local kriging to align the simulated schools with the observed catch data. Specifically, a global

variogram analysis was conducted for the catches to estimate its extent of spatial correlation, *i.e.* the distance beyond each simulated school at which the catches exhibit no dependence. The estimated extent of correlation was used to define a neighborhood around each simulated school. Optimal interpolation was conducted within the neighborhood to predict the catch at each school location. Kriging was implemented using the R package automap given the large number of simulations (Hiemstra et al., 2009).

2.6. Data analyses

Monte Carlo simulation was performed to evaluate the seven design options. For each Monte Carlo replicate $m = 1, \dots, M$, a finite population of menhaden was generated from the predicted intensity of the fitted point process models (2) and (3). Systematic random sampling was conducted based on each option $j = 1, \dots, 7$. Let B_m denote the simulated total biomass for a Monte Carlo replicate and let \hat{B}_{mj} denote the corresponding biomass estimate based on design option j . Specifically

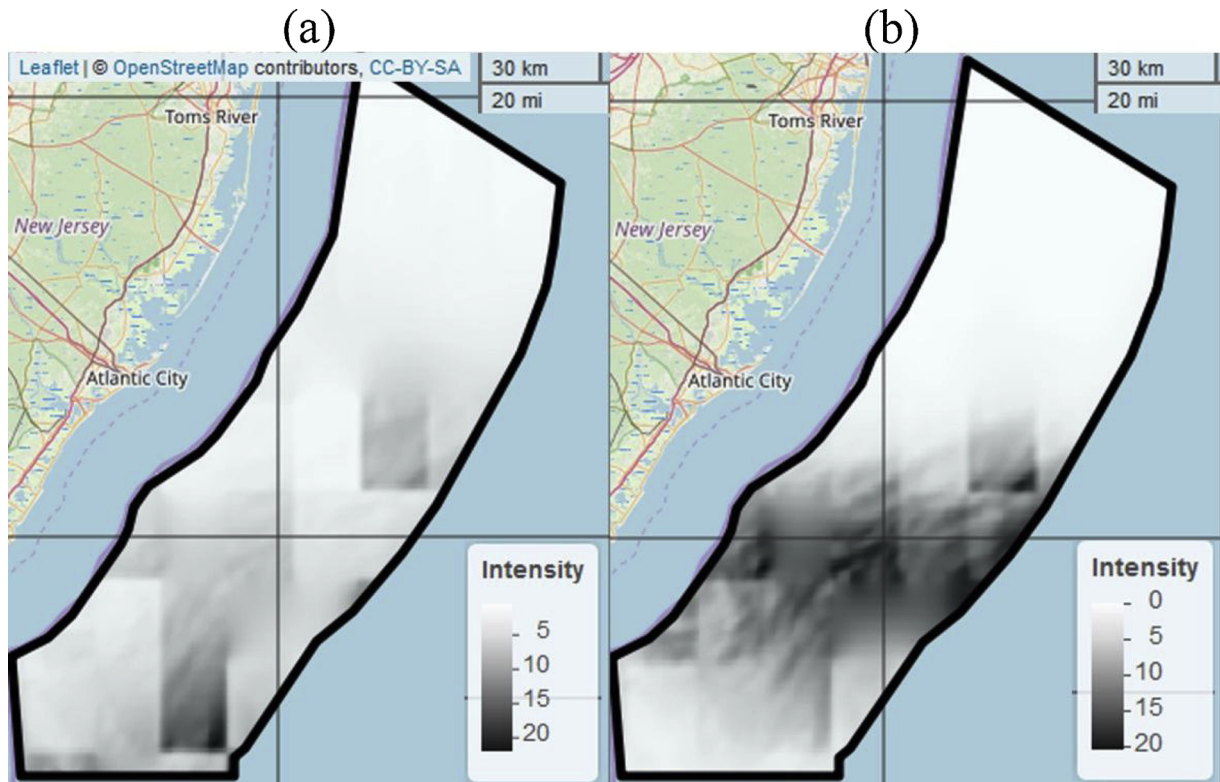


Fig. 3. Choropleth maps of spatial prediction of trip success intensity across two modeling scenarios: (a) linear effects of bathymetry, sea bottom temperature, sea bottom salinity and latitude, (b) linear effects of bathymetry and sea bottom temperature, additive effects of latitude. Intensity represents expected number of success trips per 1×1 decimal degree area, January 2017.

let y_{imj} denote the biomass at transect i and L_{imj} the corresponding transect length. Let T denote the total number of transects in the sampling frame, n denote the sample size (i.e. number of transects), and define $L = \sum_{k=1}^T L_k$, the total length of the all transects. A design-based estimator was used to obtain total biomass (4). In addition, a ratio estimator was used to incorporate the varying lengths of transects as auxiliary information (4). Given that the survey catches are likely proportional to the transect lengths, a ratio estimator can provide superior estimation to classical design-consistent estimators. The design-consistent and ratio estimators are defined as follows:

$$\hat{B}_{mj,design} = T \sum_{i=1}^n y_{imj} \text{ and } \hat{B}_{mj,ratio} = \frac{L \sum_{i=1}^n y_{imj}}{\sum_{i=1}^n L_{imj}} \quad (4)$$

The average biomass over Monte Carlo simulation B_0 was used as the true biomass. We computed the coefficient of variation (CV) as a measure of precision.

$$CV_j = \sqrt{\frac{1}{MB_0^2} \sum_{m=1}^M (\hat{B}_{mj} - B_0)^2} \text{ where } B_0 = \frac{1}{M} \sum_{m=1}^M B_m \quad (5)$$

The coefficient of variation incorporated both spatial variability of schools encountered (captured by the Poisson process model; Fig. 3) and the sampling variability (Fig. 2). Both design-based and ratio-based estimation were conducted for each sample, but the type of estimator was omitted in Eq. (5) for brevity of notation.

For comparison, the traditional preliminary estimate of necessary sampling effort was calculated based on the degree of coverage (p. 359; Simmonds and MacLennan, 2005). In this calculation, the CV was related to the total transect length sampled without considering the spatial heterogeneity of encounter rates.

$$CV_j^0 = \frac{0.5}{\sqrt{\Lambda_j}}, \Lambda_j = \frac{D_j}{\sqrt{A}} \text{ and } D_j = \frac{1}{M} \sum_{m=1}^M D_{mj} \quad (6)$$

In Eq. (6), D_j is the average total transect length sampled over

individual samples D_{mj} , and A is the survey area, Λ_j is the degree of coverage.

3. Results

We took a super-population or model-based view of sampling, which considers the variance components from both population realizations from model (1) and the randomization of the sampling units (Simmonds and Fryer, 1996). The predicted spatial patterns of encounter intensity (expected number of successful trips per unit area per winter month (Fig. 3) demonstrated the uncertainty of school responses to oceanographic conditions. The school distribution based on linear covariates showed more variability across the study area (Fig. 3a) than the patterns based on non-linear latitude effect (Fig. 3b). Both predictions exhibit increased intensity offshore near the middle of the study area. The northern part of the study area exhibited lower encounter rates.

During the 2018 winter fishing season, actual encounter rates from a fisher's logbooks were around 1 school per hour, or 0.43 schools per mile. The actual data were compared with the simulated encounter rates. The corresponding maximum number of schools encountered per transect were around 7 and 15. The re-sample sizes of 50 and 100 similar VTR trips best represented the 2018 encounter rates (Table 1). The maximum number of simulated schools per transect were between 9 and 18 with the 95% confidence intervals covering the field based estimates. The simulated total biomass represented a small proportion of the coastwide stock assessment estimate of menhaden biomass; re-sample sizes of 50 and 100 corresponded with ~15% and ~31% of the total biomass estimated in 2000, the year with lowest estimated coastwide biomass (ASMFC, 2017).

Options for down-viewing echosounder use (Option 1) and expansion of average biomass estimated from the down-viewing echosounder to schools spotted with sonar (Options 2 and 5) generated CVs between

Table 1

Simulated total biomass (metric tons) and maximum encounter rate per transect based on two Poisson process modeling scenarios: (a) linear effects of bathymetry, sea bottom temperature, sea bottom salinity and latitude, (b) linear effects of bathymetry and sea bottom temperature, additive effects of latitude. Each Poisson process modeling scenario was applied to a simulated menhaden population created using resampled Vessel Trip Report fishing trips replicated either 50 or 100 times. Six out of eighteen trips were not used due to missing temperature data ($n = 4$) or because the trip was located outside the study area ($n = 2$).

Scenario	NVTR (number of resample of VTR data = 12 trips ^a)	biomass (thou. mt)	lower 95% limit (thou. mt)	upper 95% limit (thou. mt)	maximum school per transect	lower 95% limit	upper 95% limit
(a)	50.0	86.7	80.7	93.8	9	7	12
	100.0	173.6	164.0	182.2	15	12	20
(b)	50.0	85.7	78.9	92.2	11	9	14
	100.0	171.8	162.9	181.5	18	15	22

^a Six trips not used due to missing temperature ($n = 4$) and outside area ($n = 2$) generated from SceMFS_3(total_school), result on cluster Fall2016/SceMFS.

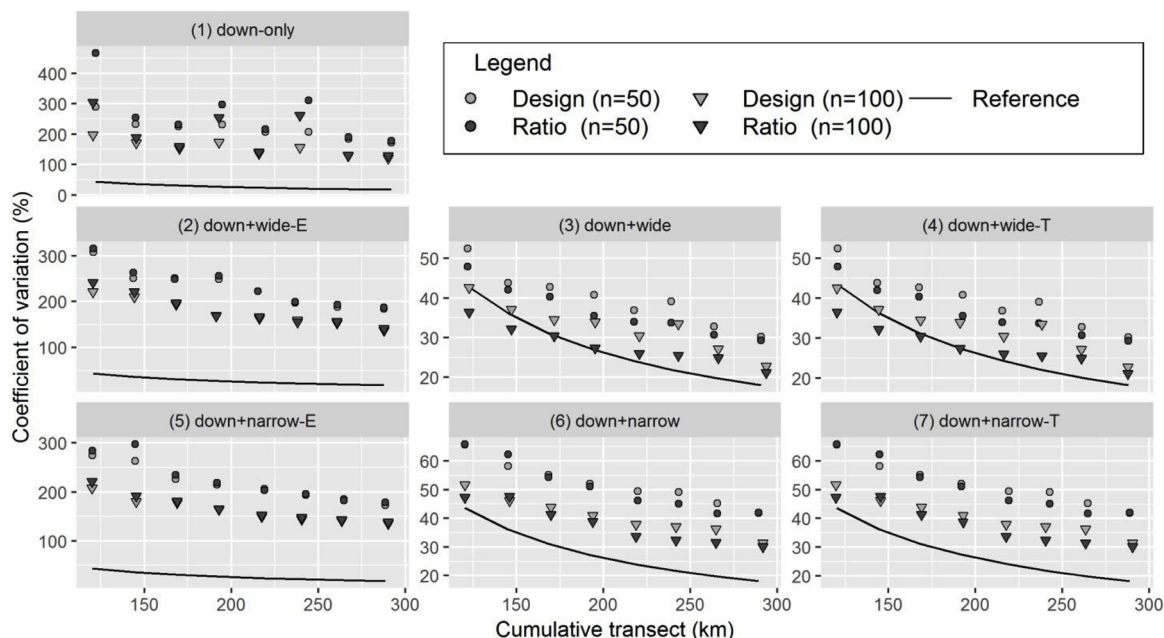


Fig. 4. Coefficient of variation based on 1999 Monte Carlo samples and the average cumulative distance sampled (km) for seven survey design options. Down-only denotes down-viewing echosounder only with 20 m swath; wide/narrow denote omni-directional sonar with 400 m/200 m detection range; down + wide/narrow denotes biomass estimated for all schools encountered by sonar via down-viewing echosounder across the omni-directional sonar detection range; E suffix denotes expansion of down-viewing echosounder biomass to all schools encountered by omni-directional sonar; T suffix denotes schools identified via omni-directional sonar and biomass determined by trawl sets. Populations were simulated based on 50 or 100 re-samples of vessel trip reports in winter 2017 based on a fitted Poisson model with linear environmental covariates. Reference lines were predictions based on the degree of coverage theory.

200% and 400% (Fig. 4). The wider detection range (option 2) was not associated with a smaller CV than the narrower detection range (option 5) because relatively few schools were observed with the down-viewing echosounder, on average, for biomass estimation. Lower CVs between 25% and 60% were generated by other options that involved both down-viewing echosounder and sonar (Options 3, 4, 6, 7; Fig. 4). The average cumulative transect distance sampled ranged between 120 km and 300 km across all options. Accuracy increased with increasing total distance surveyed. Narrower side scan swaths (200 m; Options 5–7) generated lower accuracy than wider swaths (400 m; Options 2–4) with the same survey effort. In options with high detectability for biomass (Options 3–4, 6–7), the ratio estimator that accounted for unequal transect lengths generated more accurate estimates than the design based estimator. In options with poor detectability for biomass (options 1–2,5), performance of the ratio estimator was comparable with that of the design based estimator.

Simulation-based CVs were larger than those predicted by degree of coverage theory. Simulated CVs ranged from 25% to over 400%. The 400% CV significantly exceeded the predictions from the degree of coverage theory. The extent of exceedance depended on the encounter rate, design options, and the choice of estimator. When a narrow echosounder swath width was assumed in option 1, simulated CVs were

much higher for this schooling population with sparse encounter rate. When a higher encounter rate was simulated using 100 re-samples of the VTR data (Fig. 3), survey design Options 3 and 4 (400 m swath) generated similar CVs as those predicted by degree of coverage theory (Fig. 4). The rate of change in CV per additional transect length was linear under the simulation as opposed to the super-linear decrease predicted by degree of coverage theory.

The precisions between two pairs of design options: 3 and 4, 6 and 7 were similar (Fig. 4). These pairs differed mainly in the survey costs. Qualitatively similar results (Appendix A - Figs. 2 and 3) were obtained when we simulated school intensity using an alternative fitted Poisson process model (Fig. 3b).

4. Discussion

Simulation-based CVs were larger than those predicted by the degree of coverage theory (Aglen, 1989) and used for planning acoustic surveys (Parker-Stetter, 2009; Simmonds and MacLennan, 2005), although estimates from the two approaches became more similar when the re-sample size of the population was large relative to the field-based encounter rates. This suggests that the model variance component diminishes as the population becomes less patchy, and the simulated patchiness of the

population was associated with the precision of hydroacoustic surveys. If the underlying spatial distribution is not correctly described, then the precision of acoustic surveys may be substantially lower than was designed (Barry and Welsh, 2001). Specifically, the precision of narrow swath echosounder-only surveys may generate poor biomass estimates for patchily distributed population. We expect most pelagic clupeids to exhibit non-random and patchy spatial distribution. Thus the simulation estimates of CV are comprehensive and conservative, and other approaches for designing acoustic surveys may not provide as accurate estimates of survey CV if they do not account for the patchy nature of schooling clupeids. As the population became less patchy, the traditional degree of coverage estimates were more likely to be realized. However, schools needed to occupy approximately 1.3% of the raster cells before the degree of coverage estimator was approximately correct according to the simulations herein.

The precision also depended upon the acoustics equipment. Generally, the wider the detection distance, the better the precision. The 400 m detection range assumed in Options 3 and 4 produced more precise estimates than the 200 m detection range assumed in Options 6 and 7. Although most sonar can detect schools 800–1200 m from the vessel depending on depth, bottom type, temperature, and salinity (Brehmer et al., 2007, 2006), the assumption of 400 m may be more realistic given the expected minimum distance at which schools can be reliably detected at the shallowest depths in the study area (~20 m) and the results of previous sonar surveys (Brehmer et al., 2007; Hewitt, 1976; Mackinson et al., 1999; Misund et al., 1995; Stockwell et al., 2012).

The large CV resulted from narrow detection range of the down-viewing echosounder, and the small sample size for biomass estimation. Specifically in options 2 and 5 (Fig. 4), among schools spotted by the side-scan sonar, a small fraction of them (~5–10%) were available for biomass estimation due to the narrow horizontal detection range (20 m). Thus the CVs in subpanels 2 and 5 are limited by the sample size for biomass estimation. For example, in the case where no school was observed by echosounder, biomass estimation has a sample size of zero. Thus CVs from the wide (400 m) detection range were not smaller than those from the narrow (200 m) detection range. In the other options (e.g. options 3 and 6, Fig. 4), we assumed that biomass information of all schools detected by omni-directional sonar was available for estimation, and the resulting CVs from these options are consistent with the existing designs.

Our results were consistent across several reasonable hypotheses about the spatial distribution of menhaden. The point process models included several scenarios of the environmental drivers of the menhaden distribution. Simulations with these scenarios suggest that the general conclusions regarding the CVs of the proposed acoustic survey equipment remain true. Specifically, the variance due to the stochastic distribution of the stock was incorporated in our CV in addition to the design-based variance component (Liang et al., 2017). The model variance component will likely dominate the design based component in our CV estimates when the sample size is non-negligible relative to the sampling frame (Chen et al., 2004).

In addition to the effectiveness of potential survey designs, costs are also an important factor to consider before implementation. This simulation study assumes that a vessel is available with a hull-mounted omni-directional sonar unit in addition to either a scientific echosounder or high-end industry grade equivalent. Many fishing vessels operating in the study area are equipped with long-range omni-directional sonar, but few vessels are equipped with a high-end echosounder, so there may be an additional cost. However, our results suggest the survey CV would increase dramatically when using an echosounder alone because most menhaden schools will be missed. Hence, finding ways to use a vessel that already has an omni-directional sonar (e.g., partnering with commercial fishers) may be the most cost effective approach if survey vessels are not already adequately equipped.

Simulated acoustic transect data were analyzed using a design-based and a model-based approach (ratio estimator). The model-based

approach generated more precise biomass estimates than the design-based estimator. This suggests that the unequal length of transects can be incorporated as auxiliary information in a model to reduce the statistical variability of the estimates. However, the performance of the ratio estimator depends in part on the detection range of the acoustic system. For the down-view only option, detections were sparse, and the total biomass distribution among the transects became zero-inflated. As a result, longer transects were not associated with larger total observed biomass. This problem of few observations of schools violates the assumption underlying the ratio estimator, and leads to random features observed in panel 1 and loss of efficiency for the ratio estimator observed in panels 1, 2 and 5 (Fig. 4). Additional routinely collected variables such as geographic coordinates of the samples can also provide useful auxiliary information regarding the spatial distribution of the stock. A geostatistical estimator can then incorporate this geo-spatial information to improve the precision of the abundance estimates (Jensen and Miller, 2005; Liang et al., 2017; Overholtz et al., 2006). While model-based analyses of probabilistic survey data are in general useful, they should be applied with caution to data collected by non-probabilistic survey designs (Smith, 1990). Specifically, model diagnostics and validation should be conducted to ensure that the proposed model fits the data adequately.

Some caveats to our simulation study should be noted. We assumed the biomass of all schools encountered along the transect was estimated with 100% accuracy whether captured *via* trawl or measured with an echosounder. However, midwater trawls may not always be able to capture entire schools of menhaden and there is considerable uncertainty in acoustic estimation of biomass (Simmonds and MacLennan, 2005). This uncertainty and detectability issues will need to be incorporated in the sampling design and data analyses to provide unbiased estimates. Also, an echosounder swath width of 20 m was assumed given limitations on the minimum resolution of the imagery used to spatially model menhaden school intensity. However, the actual diameter of the echosounder cone beneath the vessel will vary based on depth, salinity, and temperature (Simmonds and MacLennan, 2005). Therefore, the CV estimates generated by this simulation study should be used to weigh the relative merits of alternative survey design options and not be used as an estimate of anticipated survey estimate precision. We did not consider the survey cost in the simulation, assuming that transect distance serves as a surrogate for the total cost.

Designing a hydro-acoustic survey of menhaden remains challenging due to the highly patchy school distributions and uncertain detectability. Our simulation study indicated a traditional acoustic survey that uses a down-viewing echosounder only will not be adequate for estimating menhaden biomass across the shelf waters off New Jersey in winter given the patchy distribution of schools and the limited resources available. Only scenarios where schools are first located *via* sonar then measured *via* trawl or echosounder produced acceptable CVs (Options 3, 4, 5, 6). Our simulation results suggest that the use of down-viewing echosounder with and without the additional of omni-directional sonar and trawling would provide biomass estimates of drastically different precisions, possibly due to the patchy distribution of menhaden schools. Ideally, data from all acoustic systems would be collected and combined to account for the limitations of each equipment. Given these simulation results, we recommend a combination of down-viewing echosounder and sonar be explored as an alternative to traditional echosounder only surveys for patchily distributed schooling pelagics such as menhaden. Additionally, we recommend model-based analyses of the survey data, which should provide more accurate estimates of biomass and CV at a marginal cost of the actual survey. Our simulation based approach presented here could provide a quantitative assessment of the efficiency of given combinations of acoustic survey equipment for other stocks. If the future stock assessment of menhaden incorporates spatial structure (Tuck and Possingham, 2000; Wilberg et al., 2008), estimates of biomass in the study area could inform estimation of the magnitude of the stock.

Acknowledgements

We thank the associate editor, Dr. Joseph Warren and an anonymous referee for their helpful and constructive comments which considerably improved this paper. This project was funded by the National Science Foundation (NSF) Science Center for Marine Fisheries (SCeMFIS) under NSF award 1266057 and through membership fees provided by the SCeMFIS Industry Advisory Board. Special thanks to Stefan Axelsson, Lars Axelsson, Leif Axelsson, Lindy Barry, Micah Dean, James Gartland, Christopher Gurshin, Peter Himchak, Michael Jech, Jeff Kaelin, Ray Mroch, Wayne Reichle, and Gina Shield for contributing data and advice. This is contribution number 5715 of the University of Maryland Center for Environmental Science.

Appendix A. Supplementary data

Supplementary material related to this article can be found, in the online version, at doi:<https://doi.org/10.1016/j.fishres.2019.105402>.

References

- Aglen, A., 1989. Empirical Results on Precision-effort Relationships for Acoustic Surveys. ICES CM 1989/B: 30, 28 pp (mimeo).
- Ahrenholz, D.W., 1991. Population biology and life history of the North American menhadens, *Brevoortia* spp. Mar. Fish. Rev. 53 (4), 3–19.
- ASMFC, 2017. Atlantic Menhaden Stock Assessment Update. Arlington, VA.
- Baddeley, A., Rubak, E., Turner, R., 2015. Spatial Point Patterns: Methodology and Applications With R. 2015. URL: Chapman and Hall/CRC Press, London. <http://www.crcpress.com/Spatial-Point-Patterns-Methodology-and-Applications-with-R/Baddeley-Rubak-Turner/9781482210200/>.
- Barry, S.C., Welsh, A.H., 2001. Distance sampling methodology. J. R. Stat. Soc. Series B Stat. Methodol. 63 (1), 23–31.
- Bernasconi, M., Patel, R., Nøttestad, L., Knudsen, F., Briery, A., 2009. Use of active sonar for cetacean conservation and behavioral-ecology studies: a paradox. Proc. Inst. Acoust. 31 (1), 112–118.
- Boyd, C., Woillez, M., Bertrand, S., Castillo, R., Bertrand, A., Punt, A.E., 2014. Bayesian posterior prediction of the patchy spatial distributions of small pelagic fish in regions of suitable habitat. Can. J. Fish. Aquat. Sci. 72 (2), 290–303.
- Brehmer, P., Georgakarakos, S., Josse, E., Trygonis, V., Dalen, J., 2007. Adaptation of fisheries sonar for monitoring schools of large pelagic fish: dependence of schooling behaviour on fish finding efficiency. Aquat. Living Resour. 20 (4), 377–384.
- Brehmer, P., Lafont, T., Georgakarakos, S., Josse, E., Gerlotto, F., Collet, C., 2006. Omnidirectional multibeam sonar monitoring: applications in fisheries science. Fish Fish. Oxf. (Oxf) 7 (3), 165–179.
- Casini, M., Kornilovs, G., Cardinale, M., Möllmann, C., Grygiel, W., Jonsson, P., Raid, T., Flinkman, J., Feldman, V., 2011. Spatial and temporal density dependence regulates the condition of central Baltic Sea clupeids: compelling evidence using an extensive international acoustic survey. Popul. Ecol. 53 (4), 511–523.
- Chen, J., Thompson, M.E., Wu, C., 2004. Estimation of fish abundance indices based on scientific research trawl surveys. Biometrics 60 (1), 116–123.
- De Oliveira, J.A.A., Butterworth, D.S., 2004. Developing and refining a joint management procedure for the multispecies South African pelagic fishery. Ices J. Mar. Sci. 61 (8), 1432–1442.
- Demer, D.A., Zwolinski, J.P., Byers, K.A., Cutter, G.R., Renfree, J.S., Sessions, T.S., Macewicz, B.J., 2012. Prediction and confirmation of seasonal migration of Pacific sardine (*Sardinops sagax*) in the California current Ecosystem. Fish. Bull. 110 (1), 52–70.
- Demer, D.A., Zwolinski, J.P., Cutter Jr., G.R., Byers, K.A., Macewicz, B.J., Hill, K.T., 2013. Sampling selectivity in acoustic-trawl surveys of Pacific sardine (*Sardinops sagax*) biomass and length distribution. Ices J. Mar. Sci. 70 (7), 1369–1377.
- Diggle, P.J., 2013. Statistical Analysis of Spatial and Spatio-temporal Point Patterns. CRC Press, Boca Raton, Florida, USA.
- Fässler, S.M., Brunel, T., Gastauer, S., Burggraaf, D., 2016. Acoustic data collected on pelagic fishing vessels throughout an annual cycle: operational framework, interpretation of observations, and future perspectives. Fish. Res. 178, 39–46.
- Gimona, A., Fernandes, P.G., 2003. A conditional simulation of acoustic survey data: advantages and potential pitfalls. Aquat. Living Resour. 16 (3), 123–129.
- Hewitt, R., 1976. Development and use of sonar mapping for pelagic stock assessment in the California current area. Fish. Bull. (Wash. D. C.) 74, 281–300.
- Haugland, E.K., Misund, O.A., 2004. Evidence for a clustered spatial distribution of clupeid fish schools in the Norwegian Sea and off the coast of southwest Africa. Ices J. Mar. Sci. 61 (7), 1088–1092.
- Hiemstra, P.H., Pebesma, E.J., Twenhöfel, C.J., Heuvelink, G.B., 2009. Real-time automatic interpolation of ambient gamma dose rates from the Dutch radioactivity monitoring network. Comput. Geosci. 35 (8), 1711–1721.
- Hijmans, R.J., 2017. Raster: Geographic Data Analysis and Modeling. R Package Version 2.6-7. <https://CRAN.R-project.org/package=raster>.
- Jensen, O.P., Miller, T.J., 2005. Geostatistical analysis of the abundance and winter distribution patterns of the blue crab *Callinectes sapidus* in Chesapeake Bay. Trans. Am. Fish. Soc. 134 (6), 1582–1598.
- Jolly, G., Hampton, I., 1990. A stratified random transect design for acoustic surveys of fish stocks. Can. J. Fish. Aquat. Sci. 47 (7), 1282–1291.
- Jones, B.A., Stanton, T.K., Colosi, J.A., Gauss, R.C., Fialkowski, J.M., Jech, J.M., 2017. Broadband classification and statistics of echoes from aggregations of fish measured by long-range, mid-frequency sonar. J. Acoust. Soc. Am. 141 (6), 4354–4371.
- June, F.C., Reintjes, J.W., 1959. Age and Size Composition of the Menhaden Catch Along the Atlantic Coast of the United States, 1952-55: With a Brief Review of the Commercial Fishery. US Department of Interior, Fish and Wildlife Service.
- Kalikhman, I., Ostrovsky, I., 1997. Patchy distribution fields: survey design and adequacy of reconstruction. ICES J. Mar. Sci. 54 (5), 809–818.
- Latour, R., 2013. Survey Design for Adult Atlantic Menhaden along the U.S. East Coast. Virginia Institute of Marine Science, Gloucester Point, VA.
- Liang, D., Nessler, G., Wilberg, M.J., Miller, T.J., 2017. Bayesian calibration of blue crab (*Callinectes sapidus*) abundance indices based on probability surveys. J. Agric. Biol. Environ. Stat. 22 (4), 481–497.
- Liljestrand, E.M., Wilberg, M.J., Schueller, A.M., 2019. Estimation of movement and mortality of Atlantic menhaden during 1966–1969 using a Bayesian multi-state mark-recovery model. Fish. Res. 210, 204–213.
- Lucca, B.M., Warren, J.D., 2018. Acoustically measured distribution and abundance of Atlantic menhaden (*Brevoortia tyrannus*) in a shallow estuary in Long Island, NY. Estuaries and coasts 41 (5), 1436–1447.
- Lucca, B.M., Warren, J.D., 2019. Fishery-independent observations of Atlantic menhaden abundance in the coastal waters south of New York. Fish. Res. 218, 229–236.
- Mackinson, S., Nøttestad, L., Guénette, S., Pitcher, T., Misund, O., Fernø, A., 1999. Cross-scale observations on distribution and behavioural dynamics of ocean feeding Norwegian spring-spawning herring (*Clupea harengus* L.). ICES J. Mar. Sci. 56 (5), 613–626.
- Misund, O.A., Aglen, A., Frønæs, E., 1995. Mapping the shape, size, and density of fish schools by echo integration and a high-resolution sonar. ICES J. Mar. Sci. 52 (1), 11–20.
- Overholtz, W., Jech, J.M., Jacobson, L., Sullivan, P., 2006. Empirical comparisons of survey designs in acoustic surveys of Gulf of Maine-Georges Bank Atlantic herring. J. Northw. Atl. Fish. Sci. 36, 127–144.
- Parker-Stetter, S.L., 2009. Standard operating procedures for fisheries acoustic surveys in the Great Lakes. Great Lakes Fish. Comm. Spec. Pub 09-01.
- Reintjes, J.W., 1969. Synopsis of Biological Data on the Atlantic Menhaden, *Brevoortia tyrannus*. US Bureau of Commercial Fisheries.
- Richaud, B., Kwon, Y.O., Joyce, T.M., Fratantoni, P.S., Lentz, S.J., 2016. Surface and bottom temperature and salinity climatology along the continental shelf off the Canadian and US East Coasts. Cont. Shelf Res. 124, 165–181.
- SEDAR, 2015. SEDAR 40 – Atlantic Menhaden Stock Assessment Report. SEDAR, North Charleston SC. 643 pp. available online at: http://www.sefsc.noaa.gov/sedar/Sedar_Workshops.jsp?WorkshopNum=40, (North Charleston, SC).
- Simmonds, E.J., 1996. Survey design and effort allocation: a synthesis of choices and decisions for an acoustic survey. North sea herring is used as an example. ICES J. Mar. Sci. 53, 285–298.
- Simmonds, E.J., Fryer, R.J., 1996. Which are better, random or systematic acoustic surveys? A simulation using North Sea herring as an example. ICES J. Mar. Sci. 53 (1), 39–50.
- Simmonds, E.J., MacLennan, D., 2005. Fisheries Acoustics. Chapman & Hall, London.
- Simpson, C., Bi, H., Liang, D., Wilberg, M.J., Schueller, A., Nessler, G., Walsh, H., 2017. Spawning locations and larval dispersal of Atlantic menhaden during 1977–2013. ICES J. Mar. Sci. 71 (6), 1574–1586.
- Simpson, C., Wilberg, M.J., Bi, H., Schueller, A., Nessler, G., Walsh, H., 2016. Trends in relative abundance and early life survival of Atlantic menhaden during 1977–2013 from long-term ichthyoplankton programs. Trans. Am. Fish. Soc. 145 (5), 1139–1151.
- Smith, J.W., 1991. The Atlantic and gulf menhaden purse seine fisheries: origins, harvesting technologies, biostatistical monitoring, recent trends in fisheries statistics, and forecasting. Mar. Fish. Rev. 53 (4), 28–41.
- Smith, S.J., 1990. Use of statistical models for the estimation of abundance from groundfish trawl survey data. Can. J. Fish. Aquat. Sci. 47 (5), 894–903.
- Stockwell, J.D., Weber, T.C., Baukus, A.J., Jech, J.M., 2012. On the use of omnidirectional sonars and downwards-looking echosounders to assess pelagic fish distributions during and after midwater trawling. ICES J. Mar. Sci. 70 (1), 196–203.
- Thompson, S.K., 2012. Sampling, 3rd ed. Wiley, Hoboken, New Jersey.
- Tuck, G.N., Possingham, H.P., 2000. Marine protected areas for spatially structured exploited stocks. Mar. Ecol. Prog. Ser. 192, 89–101.
- Wilberg, M.J., Irwin, B.J., Jones, M.L., Bence, J.R., 2008. Effects of source-sink dynamics on harvest policy performance for yellow perch in southern Lake Michigan. Fish. Res. 94 (3), 282–289.
- Wood, S.N., 2011. Fast stable restricted maximum likelihood and marginal likelihood estimation of semiparametric generalized linear models. J. R. Stat. Soc. Ser. B 73 (1), 3–36.
- Zwolinski, J.P., Demer, D.A., Byers, K.A., Cutter, G.R., Renfree, J.S., Sessions, T.S., Macewicz, B.J., 2012. Distributions and abundances of Pacific sardine (*Sardinops sagax*) and other pelagic fishes in the California current Ecosystem during spring 2006, 2008, and 2010, estimated from acoustic-trawl surveys. Fish. Bull. 110 (1), 110–122.